High-resolution *in situ* measurement of nitrate in runoff from the Greenland Ice Sheet

Authors: Alexander D. Beaton[1], Jemma L. Wadham[2], Jon Hawkings[2], Elizabeth A. Bagshaw[3], Guillaume Lamarche-Gagnon[2], Matthew C. Mowlem[1,] Martyn Tranter[2]

1. National Oceanography Centre, European Way, Southampton, SO14 3ZH
2. Bristol Glaciology Centre, University of Bristol, University Road, Bristol, BS8 1SS
3. School of Ocean and Earth Sciences, Cardiff University, Cardiff, CF10 3AT

*Corresponding author: a.beaton@noc.ac.uk, Tel: +442380596268

Abstract

We report the first *in situ* high-resolution nitrate time series from two proglacial meltwater rivers draining the Greenland Ice Sheet, using a recently developed submersible analyser based on lab-on-chip (LOC) technology. The low sample volume (320 μL) required by the LOC analyser meant that low concentration (few to sub μM), highly turbid subglacial meltwater could be filtered and colourimetrically analysed *in situ*. Nitrate concentrations in rivers draining Leverett Glacier in South-West Greenland and Kiattuut Sermiat in Southern Greenland exhibited a clear diurnal signal and a gradual decline at the commencement of the melt season, displaying trends that would not be discernible using traditional daily manual sampling. Nitrate concentrations varied by 4.4 μM (+/- 0.2 μM) over a 10-day period at Kiattuut Sermiat and 3.0 μM (+/- 0.2 μM) over a 14 day period at Leverett Glacier. Marked changes in nitrate concentrations were observed when discharge began to increase. High resolution *in situ* measurements such as these have the potential to significantly advance the understanding of nutrient cycling in remote systems, where the dynamics of nutrient release are complex but are important for downstream biogeochemical cycles.

TOC art

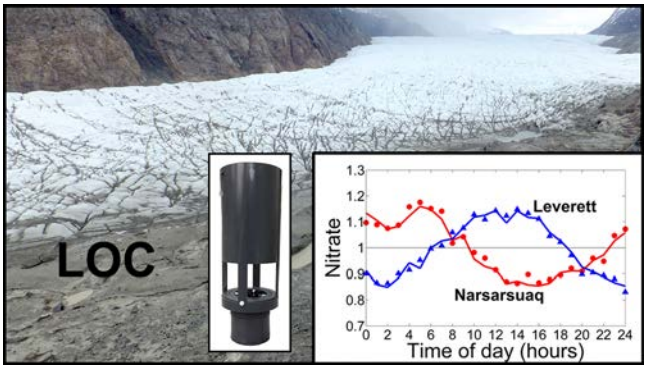

Introduction

There is now a growing body of evidence to suggest that glacial environments are active and significant components of the global nitrogen cycle. Evidence exists for nitrification and nitrogen fixation on glacier surfaces [1,2], while both nitrification and nitrate reduction [3,4] have been shown to occur in subglacial sediments. Export of nitrogen from ice sheets through glacial meltwater may fertilise downstream marine ecosystems [5], potentially helping to support the presence of near-ice blooms [6] and high rates of primary production [7] around the Greenland Ice Sheet. Annual dissolved inorganic nitrogen flux from the Greenland Ice Sheet has been estimated at 30-40 Gg [5], which is comparable to large Arctic rivers yet supplies different ocean basins.

To date, the measurement of nutrients in glacial meltwater has taken place exclusively through the manual collection of discrete samples and subsequent laboratory-based analysis (typically through automated colourimetric methods (e.g. [1]) or ion chromatography (e.g. [3,5,8]). This approach is expensive and time-consuming, and results in sporadic and/or low temporal-resolution datasets. Hence, the chemistry of glacial meltwater, including that reaching the polar oceans, is chronically under-sampled, and information on processes involved in nutrient cycling is lacking. This is likely to have important consequences for the accuracy of estimated nutrient fluxes from ice sheets and glaciers into the fjords and polar oceans [9], and also on predictions about how climate-driven changes in ice-sheet run-off might influence downstream primary production [8].

High-resolution, quasi-continuous *in situ* measurements enable better understanding of nutrient fluxes and temporal dynamics in glacial systems. *In situ* sensors and analysers can be deployed in remote and inaccessible locations where traditional manual sampling techniques would be logistically difficult and potentially dangerous. There have so far been few applications (e.g. [10]) of *in situ* chemical sensors to the measurement of glacial meltwater, and none for the measurement of nitrate and other nutrients. The harsh ambient environmental conditions, high sediment loads and low concentrations found in glacial environments are a challenge for conventional sensor technologies [11].

Several studies to date (e.g.[12–14]) have used UV absorbance nitrate sensors to conduct high temporal resolution *in situ* measurements in freshwater streams and rivers. UV absorbance sensors require no reagents, and have been deployed for extended periods (several months). Nitrate concentrations are typically sub- to low μM in glacial meltwaters [3,5,15], hence the relatively poor limit of detection (LOD) - e.g. 0.5 μM for SUNA V2 - and accuracy (e.g. +/- 2 μM for SUNA V2) make UV absorbance systems largely unsuitable. Likewise, ion selective electrodes have been used in rivers to measure nitrite and nitrate [16,17], but poor LOD (e.g. 0.5 μM) and drift make them unsuitable for pristine glacial environments.

Reagent based colourimetric analysers offer an alternative technology for *in situ* measurement of nitrate, and several other parameters (e.g. [18–21]). These systems miniaturise standard laboratory-based analysis techniques, and have been deployed in rivers, estuaries [22], marine environments [23], and more recently in an oligotrophic arctic stream [24]. The creation of an absorbing dye, with highly specific reagents, produces a robust and sensitive measurement technique, resulting in high precision and lower LODs. Furthermore, the ability to carry and analyse on-board standards leads to high-accuracy measurements and drift correction. Standard wet chemical (reagent) assays have been adapted to *in situ* use for a number of biogeochemical parameters, such as nitrate, nitrite, ammonia, phosphate and dissolved iron. Despite these advantages, reagent based sensors are typically large and bulky, and consume large amounts of power and reagents, making them unsuitable for remote long-term operation, especially in remote environments.

Recent work has shown that *in situ* reagent-based colourimetric sensors can be enhanced using microfluidics [25,26]. Implemented through lab-on-a-chip (LOC) technology, microfluidics (the manipulation of small volumes of fluids through microchannels, typically tens to hundreds of μm wide) allows reduced reagent consumption, lower power consumption and a decrease in the physical size and weight of chemical analysis systems. This development has the potential to expand the applicability of *in situ* colourimetric analysers to a wide variety of deployment scenarios that were unsuitable for the previous generation of systems. The measurement of glacial meltwater is a prime example.

Glacial environments present a unique set of challenges for the application of *in situ* chemical analysis systems, including high suspended sediment loads, low analyte concentrations, low ambient temperatures, remote deployment locations and the necessity for stand-alone low-power operation. Glacier runoff is highly turbid (e.g. up to 13.1 g/l [27]), presenting problems for optical measurement systems and filters. However, microfluidic systems use low sample volumes (in this case ~320 μL), allowing proglacial meltwater to be filtered to the point that it is optically clear and free of particles (>0.45 μm) without requiring excessive filter changes. Low fluid volumes mean that less energy is spent on pumping, typically the main power-draw in fluidic analysers [26], resulting in low power consumption, which is essential for remote deployment. Remote locations also mean that sensors may need to be carried on foot to deployment sites, making lightweight, portable devices (such as microfluidic sensors) essential.

Here, we report the first applications of a microfluidic LOC colourimetric sensor for the *in situ* measurement of nitrate in meltwater rivers draining the Greenland Ice Sheet. This work represents the first measurement of nitrate *in situ* and at high temporal resolution in glacial runoff. The limit of detection (0.025 μM) and range (0.025 to 350 μM) of the system are adequate and suitable for the nitrate concentrations measured in the glacial runoff, and the power consumption (1.8 W) is low enough that the analyser can be deployed in remote locations with power provided by a solar-charged battery.

Materials and Methods

Field sites

LOC analysers were deployed to measure runoff emerging from two contrasting outlet glaciers of the Greenland Ice Sheet.

The first deployment was from 26th May to 6th June, 2013, in runoff emerging from Kiattuut Sermiat (KS, 61.2N, 45.3W, Figure 1A), a land terminating outlet glacier of the Greenland Ice Sheet located ~8 km from Narsarsuaq in southern Greenland (Figure 1A), estimated to cover an area of 36 km^2 [28]. Subglacially derived meltwater emerging from the glacier discharges into a proglacial lake, ~ 0.5 km^2 and 12 m deep at its centre [29], which in turn flows into a proglacial river (the Kuusuaq river) leading into the fjord. The LOC analyser was deployed at a site approximately 1 km downstream of the lake, and was programmed to take a measurement of nitrate plus nitrite (referred to here as ΣNO_x) approximately every 20 minutes.

The second deployment was from 26th May to 9th June, 2015, in runoff emerging from Leverett Glacier (LG, 67.06N, 50.17W, Figure 2B). LG is a large polythermal-type land terminating outlet glacier in west Greenland draining a catchment area ~600 km^2 [30]. Meltwaters emerge from a well-defined portal located on the northern side of the glacier terminus. The resultant proglacial river flows downstream into the Watson River, which eventually enters Sondre Stromfjord. The large catchment is hydrologically and geologically [28] representative of a large area of the Greenland Ice Sheet, which, combined with the single well defined meltwater river, makes LG a more suitable site for studying nutrient export dynamics. The analyser at LG was programmed to perform a ΣNO_x measurement every 1hour.

LOC analyser

The LOC system performs automated colourimetric ΣNO_x analysis on a polymer microfluidic chip using the Griess assay and cadmium reduction [25]. The chip contains a network of microchannels (dimensions 150 μm x 300 μm) and two sequential on-chip optical absorption cells (2.5 mm and 25 mm in length). The analyser has a limit-of-detection of 0.025 μM and a linear dynamic range up to 350 μM. Fluid

handling is performed by a custom-built three-channel syringe pump and fourteen solenoid valves attached directly to the chip, and the system is controlled using a custom microcontroller-based electronics package. The development and first deployments of the LOC analyser have been described previously [25,31].Two different deployment and filtering set-ups were used in this experiment. At KS, the LOC sensor was housed in a water-tight Perspex tube mounted in a plastic box on the bank beside the proglacial river. The shallow depth of the water meant that the sensor was kept on the riverbank, and water was delivered to it using a lift pump and dual filtering system. At LG, where the channel was deeper, the sensor was housed in a PVC tube, and submerged so that the filter inlet was below the waterline. A single 0.45 μm inline syringe filter with prefilter (Millex-HPF PTFE, Merck Millipore) was used at the inlet to the sensor. The sensor housings were placed in perforated plastic boxes which were weighed down with rocks collected from the shoreline.

Reagents, calibration standards and collected waste were stored in 500 ml Flexboy bags (Sartorius-Stedim). All liquid that passed through the system was collected as waste, ensuring that no chemical waste from the analyser (including that which passed through the cadmium reduction tube) entered the environment. The system operated at a flow rate of 165 μL/min (per syringe). Each measurement was accompanied by a blank measurement (MilliQ water) and the measurement of a 3 μM nitrate standard, allowing continuous calibration throughout the deployment, thus compensating for changes in ambient temperature. Reagents and standards were prepared as described previously [25]. Blank and standard solutions were fixed using 0.01% chloroform. Analytical uncertainties in the measurements performed by the LOC analyser were estimated by calculating twice the running standard deviation (n = 5) of the measurements of the 3 μM standard [32] and averaging for the deployment period.

Lift pump

At KS, a miniature peristaltic pump (100 series, Williamson Manufacturing Company Limited), mounted in a water-tight box next to the sensor, was used to lift proglacial meltwater from the stream up to a t-piece mounted at the input via a 4.3 m long R-3603 Tygon tube (1.6 mm internal diameter). The pump

operated at a flow rate of 1.4 mL/min, resulting in an 8 minute delay between water leaving the proglacial stream and reaching the t-piece. The flow rate was chosen as a compromise between minimising both the amount of high-turbidity water passing through the cross-flow pre-filter in the river (see below), and the delay between water leaving the proglacial river and reaching the analyser. A cross-flow pre-filter was placed in the river at the entrance to the Tygon tubing. The pre-filter was created by slicing open a 50 mm diameter MILLEX-GP (Merck Millipore) filter unit, removing the 0.22 μm pore-size filter membrane and replacing it with a 1 μm pore size filter membrane. The outside edge of the filter membrane was secured to the inside of one half of the filter unit using Araldite epoxy, and the remaining half of the filter unit was discarded. This created an open-faced cross-flow filter (Figure 2B) which was placed into the proglacial stream, where the flow of water helped clean the exposed face of filter. Pre-filtered meltwater subsequently passed through an inline 0.45 μm Millex-HP (PES membrane, Merck Millipore) filter on entrance to the LOC analyser.

Manually collected samples

At KS, two independent sets of manually collected proglacial stream nutrient samples were taken during the sensor deployment period. These were filtered through 0.45 μm syringe filters and frozen for later analysis [5]. One set was analysed using a QuAAtro segmented flow analyser, and the other was analysed using a Thermo Scientific Dionex Ion Chromatograph ICS5000+ Capillary system with IonPac AS-11 HC anion-exchange column. In addition, six supraglacial stream samples were taken from meltwater entering moulins close to the ice margin (analysed using ion chromatography as above). At LG, one set of samples was filtered (0.45 μm), frozen, and analysed colourimetrically using a Thermo Gallery and the hydrazine reduction method (precision based on five replicates of a 1.42 μM standard was +/- 1.1%, accuracy was + 4.2%). A second set of samples was filtered (0.45 μm), stored chilled, and analysed using ion chromatography (as above).

Additional sensors

Sensors for water temperature (Campbell 247 at KS and Aanderaa 3830 at LG), electrical conductivity (EC) (Campbell 247) and pH (Honeywell Durafet, temperature compensated) were deployed alongside the LOC sensor and linked to Campbell CR1000 loggers located in plastic housings on the riverbanks. An additional station (approximately 150 m downstream) recorded air temperature (Campbell 107), water stage (Druck pressure transducer) and photosynthetically active radiation (PAR) at KS. For part of this deployment, an oxygen optode (Aanderaa 3830) was deployed approximately 200 m upstream from the LOC analyser. Sensors for PAR and dissolved oxygen (Aanderaa 3830) were co-located with the LOC analyser and operated for the duration of the deployment at LG. Fluorometric dye (Rhodamine-WT) traces conducted at a wide variety of water levels were used to convert water stage measurements into meltwater discharge values at both sites[33,34] using previously published methods[30] (see Supporting Information for additional details on discharge measurements).

The LOC analyser, lift pump and additional sensors and loggers were all powered by a 20 Ah solar-charged absorbent glass mat (AGM) lead acid battery mounted in a waterproof box beside the river.

Results

Kiattuut Sermiat (KS)

The LOC analyser recorded ΣNO_x concentrations in the proglacial stream over a 10-day period (Figure 3A). ΣNO_x averaged 3.64 µM +/- 0.2 µM, and varied between 1.39 and 5.79 µM (+/- 0.2 µM). During this period, water temperature (Figure 3B) varied between 1.16 and 3.15 °C (+/- 0.4 °C) and air temperature (Figure 3B) between 1.5 and 15.2 °C (+/- 0.4 °C). Electrical conductivity (Figure 3C) varied between 46.2 and 50.6 μScm^{-1} (+/- 10%) and pH (Figure 3D) between 7.77 and 8.26 (+/- 0.1). An equipment failure meant that dissolved oxygen data (Figure 3C) is only available from the first three days of deployment, but this showed variations between 102.7 and 114.2 % (+/- 2.5 %) of air saturation.

188 Clear diurnal cycles in ΣNO_x concentration were observed. Days 1 to 4 show a slight downward trend
189 (average decrease of 0.31 µM per day), with a mean value of 3.73 µM and diurnal variations with a mean
190 amplitude of 1.27 µM. Hydrological conditions were relatively stable during this period, with discharge
191 averaging 7.33 $m^3 s^{-1}$ (+/- 12%) and increasing slowly (by 0.27 $m^3 s^{-1}$ per day) while exhibiting average
192 daily cycles of 1.16 $m^3 s^{-1}$ in amplitude. pH showed diurnal variations (amplitude of pH 0.24), as did
193 water temperature (1.4 °C) and EC (0.74 μScm^{-1}). Elevated night-time temperatures on Day 153 marked
194 the beginning of a large increase in discharge, which was associated with a drop in conductivity and
195 dampening of diurnal pH cycles. This coincided with an increase in the amplitude of daily ΣNO_x
196 concentrations, which on the final two days peaked at 5.79 µM and dropped to 1.39 µM. Discharge
197 reached 31.4 $m^3 s^{-1}$ by the end of the deployment period and was continuing to rise. Nitrite (NO_2^-) made
198 up no more than 1.8% of the ΣNO_x signal in collected water samples (mean=1.14%, n=14), showing that
199 the ΣNO_x signal was dominated by nitrate (NO_3^-). There was a visible build-up of sediment on the face of
200 the cross-flow filter, yet the pre-filtering system was able to continuously deliver a 1 µm pre-filtered
201 sample stream to the analyser for the duration of the deployment. However, sediment build-up on the
202 surface of the pre-filter caused gas bubbles to appear in the sample stream because of sample outgassing
203 at the reduced pressure between the filter and the pump. Occasionally, a bubble would be drawn into
204 analyser, resulting in an anomalous reading. Out of the 386 ΣNO_x measurements conducted by the
205 analyser at KS, 31 (<10 %) were excluded due to the presence of bubbles drawn in through the sample
206 inlet. Gaps in the dataset from KS were caused by a fault with the sensor pump, which was subsequently
207 identified and fixed, preventing reoccurrence on subsequent deployments.

208 **Leverett Glacier (LG)**

209 The LOC analyser operated continuously over a 14 day period, recording ΣNO_x concentrations between
210 0.96 and 3.98 µM (+/- 0.2 µM) (Figure 4A) and yielding a much more complete dataset that that achieved
211 at KS. Conductivity ranged from 5.45 to 44.55 µS cm^{-1} (+/- 10%) (Figure 4B), pH from 6.45 to 7.31 (+/-

0.1) (Figure 4D) and DO from 93.10 to 102.3 % (+/- 2.5 %) of air saturation (Figure 4B). Air temperature dropped to as low as -3.22 ºC and reached a maximum of 12.0 ºC, while water temperature ranged from 0.02 to 4.41 ºC (Figure 4C). ΣNO_x concentrations showed a gradual downward decline over the first six days (0.31 µM per day). High air temperatures on Day 151 prompted a sharp increase in discharge, which was followed by a gradual increase in ΣNO_x concentration for the remaining eight days. A clear diurnal signal in ΣNO_x concentrations was recorded again (mean amplitude 0.75 µM), peaking at 14:00 and reaching a trough at 02:00. Manual samples were collected at higher temporal resolution than at KS (up to 3 times per day), and show good agreement with the LOC sensor, allowing us to validate the short-term variations measured by the sensor (Figure 4A). LG exhibited strong diurnal cycles in conductivity (average amplitude of 13.30 µS cm^{-1}) compared to KS, where the diurnal conductivity cycles were less pronounced (average amplitude <1 µS cm^{-1}). Water temperature exhibited a sharp increase (of up to 4ºC) during the day and returned to a background level of ~0.1ºC during the night. Diurnal cycles of both water temperature and oxygen saturation were dampened as discharge increased toward the end of the deployment period. We found that it was not necessary to change the filter for the duration of the deployment at LG, despite not using the lift-pump and cross-flow filter setup. Out of 321 measurements conducted by the LOC sensor during the 14 day period, 10 were removed as outliers.

Linear regression analysis shows strong correlation between the frozen samples that were analysed colourimetrically and the measurements performed by the LOC sensor (LOC = (0.95 +/- 0.17)*sample + 0.04 +/- 0.4, $p<0.05$, $R^2 = 0.82$, n = 33; Supporting Information Figure S1). There is no systematic offset, and the linear regression fit between the LOC sensor and samples is not statistically different to a 1:1 line. Despite demonstrating similar trends, the non-frozen samples (analysed using ion chromatography) show a less convincing statistical agreement with the LOC sensor (LOC = (0.65 +/- 0.22) *sample + 0.9 +/- 0.5, $p<0.05$, $R^2 = 0.57$, n = 29; Supporting Information Figures S1 and S2), which could potentially be due to sample degradation during storage.

Diurnal trends

The daily cycle for each of the measured parameters during both deployments is compared in Figure 5. Each value was normalized to the average for that value during the 24-hour period in which it was measured. Mean and median values for these normalized data were calculated for each hour, and plotted over a single 24 hour period. Data shown is for the full deployment period at LG and for the hydrologically stable period before Day 153 (where there are fewer gaps in the data) at KS.

Diurnal cycles for the measured physical parameters (air temperature, water temperature and PAR) display similar properties at KS and LG, although at LG water temperature has no defined trough and stays low (close to zero – Figure 4C) between 0:00 and 06:00. However, there are marked differences between KS and LG for several of the other measured chemical parameters, including ΣNO_x. ΣNO_x concentrations peaked at 05:00 and reach a minimum at 15:30 at KS, while they peaked at 14:00 and reached its minimum at 02:00 at LG. At KS, conductivity reached its peak at 07:00 and its trough at 17:00, while at LG conductivity peaked at 12:00 at reached its minimum at 21:00. The peak in water level/discharge occurs slightly earlier at LG (20:00) compared to KS (23:00). At LG, pH followed a similar trend to conductivity, peaking at 11:00 and reaching its minimum at 21:00, while at KS pH peaked at 12:00 and reached its minimum at 0:00. At KS, DO saturation shows approximately the opposite trend to ΣNO_x, peaking at around 15:00 and reaching a minimum at 5:00, while at LG DO saturation peaked at 13:00 and reached its lowest at midnight.

Discussion

The datasets described here represent the first high-resolution measurements of nitrate in melt waters draining the Greenland Ice Sheet, and are also the first high-resolution nutrient data for glacial systems. The LOC analysers resolved temporal dynamics of nitrate concentrations in proglacial rivers, revealing the presence of diurnal cycles and short term trends, which were verified using sub-daily manual sampling. The LOC analyser is a viable monitoring tool in this highly challenging environment.

Nitrate concentrations in glacial runoff varied by up to 4.4 μM over a 10-day period at KS and 3.0 μM over a 14 day period at LG. This variability has not been captured by manual sampling to date, which enables more accurate estimation of nutrient export from glaciated areas due to the removal of potential bias when single, daily samples are collected at approximately the same time.

There are multiple factors that influence the nitrate concentrations in proglacial rivers draining the Greenland Ice Sheet, including the source of water (primarily snowmelt and ice melt), water flow paths (e.g. via subglacial and groundwater environments), the leaching of potential N-reservoirs (e.g. leaching of snowpack, soils and subglacial debris), and microbial processes along and within the flow paths, which may act as sinks or sources of nitrate [5].

High resolution chemical trends at Kiattuut Sermiat

Clear diurnal cycles in the nitrate concentrations at KS are superimposed on a trend of slightly declining concentration over the first four days (Figure 3a). EC values (~50 μS/cm) vary inversely with diurnal discharge (Figures 5e and g), although the diurnal variation is much less pronounced than at LG (<1 μS cm^{-1} compared to >10 μS cm^{-1}). This suggests minimal influence of daily meltwater inputs on diurnal variability in the stream, possibly due to a dampening effect by the proglacial lake. At this early stage in the melt season an efficient channelised subglacial drainage system had not yet developed [33], and the lake was likely being fed by a combination of local snowmelt, supraglacial runoff, and small subglacial inputs from distributed drainage pathways. Biogeochemical processes in the proglacial lake were likely able to influence control over nutrient concentrations in the runoff.

Dissolved oxygen in the river was continually above 100% air saturation (Figure 3C) and fluctuated strongly on a daily basis, indicating an additional oxygen source within the proglacial stream or lake. Algal growth was observed in the stream and lake (visible on the sensor photographs in Figure 2B). Minimum daily concentrations of nitrate coincided maximum readings for PAR, DO and pH (Figure 5 a, b, c and f), suggesting that photosynthesis in the surface lake waters had a first order control on diurnal

variations in nitrate. Observations of highest nitrate concentrations in early morning and lowest nitrate concentrations in the late afternoon are consistent with several other studies that have attributed nitrate fluctuations in streams to autotrophic production [12,35,36].

Assuming the daily cycle in nitrate (mean amplitude 1.27 μM) was entirely a result of autotrophic assimilation and using a stoichiometric C:N ratio of 6.6:1, the carbon uptake rate due to primary production is estimated to be 8.4 mmol C $m^{-3}d^{-1}$ (79.5 mg C $m^{-3}d^{-1}$). This is similar to the assimilation rate estimated during a similar study in an oligotrophic Arctic steam (10.8 mmol C m^{-3} d^{-1} [24], assuming a 12-hour photoperiod), and on the lower end of reported ranges for large rivers of the world (0 - 132 mmol C $m^{-3}d^{-1}$, reviewed by [37] and converted to daily rates assuming a 12 hour photoperiod). Lack of light penetration would impede primary production in highly turbid proglacial streams.

EC fell more rapidly when discharge increased after Day153, and while maximum daily nitrate concentrations persisted at 5 μM, minimum daily concentrations decreased from ~3 μM to 1 μM. Decreases in nitrate as discharge increased are likely either associated with dilution from the connection of a low-nitrate water source (e.g. increased supraglacial icemelt or the draining of an ice-marginal lake), or an increased nitrate sink (e.g. increased productivity) in the lake and river system. Supraglacial waters were all highly depleted in nitrate (mean = 0.08 μM, SD = 0.05 μM, n = 6, see Supporting Information Table S1) compared to concentrations in the proglacial river, and would therefore have a diluting effect on proglacial stream nitrate concentrations.

High resolution chemical trends at Leverett Glacier

Clear diurnal cycles were also evident in the nitrate concentrations at LG (Figure 4a). These were superimposed on a trend of slightly declining concentration over the first six days. A major difference with KS is that maximum daily nitrate concentrations at LG coincided with maximum DO, PAR and pH (Figure 5 a, b, c and e), strongly suggesting that photosynthesis was not a first order control on diurnal variations in nitrate at LG. Here, where there is no proglacial lake and EC variations are much more

pronounced, diurnal variations in nitrate are more likely a result of dilution by the daily meltwater inputs. The daily peak in nitrate is coincident with the peak in conductivity, which occurs at low flow, whereas high flow is coincident with the troughs in pH and conductivity. Dilute low-pH water is an indicator of fresh snowmelt (e.g. [38,39]). The inferred fresh snowmelt pulse appears to be depleted in nitrate, while the peak in nitrate is associated with higher EC, more concentrated water. Bulk snowmelt concentrations have been previously recorded in this area as 1.03 +/- 0.30 μM [2]. Rather than coming from the fresh daily pulse of snowmelt, the daily nitrate peaks likely reflect groundwater enriched in nitrate (e.g. through microbial nitrification) [40–42]), which is then diluted by the fresh daily pulse of snowmelt. A marked increase in discharge occurred on Day 152 coincided with a switch from decreasing to increasing nitrate concentrations, which may be the influence of early subglacial meltwater. The evolution of the subglacial drainage system from an inefficient system draining mostly overwinter stored waters to a more efficient system allowing surface melt to transit rapidly at the glacier bed was not observed until day 170 (see [34]). Hence, any runoff derived from the subglacial drainage system during the monitoring period (prior to Day 170) is composed of long residence time distributed system waters that have likely been in storage at the glacier bed over winter. Subglacial environments are viable habitats for microbial life [43,44], and previous studies have reported microbial-driven nitrate production [3,4] through nitrification of surface derived ammonium in subglacial environments (this would require some oxygen to be present in the subglacial system, potentially supplied via basal melting). There is also a potential geological source of ammonium through rock comminution (e.g. [45–47]) which could then undergo nitrification. These processes could enrich early subglacially derived meltwater with nitrate (e.g. [5]), and potentially explain the rise in nitrate levels as discharge increases after Day 152. More concentrated subglacial waters and groundwater continued to be diluted by fresh snowmelt during the day, explaining the continued diurnal nitrate signal.

Diurnal nitrate signals measured with *in situ* sensors have been reported previously for snowmelt streams, and these have been attributed to either autotrophic uptake [14] or increased soil water inputs [24]. This paper reports the use of a novel *in situ* instrument to produce the first high-resolution automated nutrient

measurements in glacial meltwater streams, in association with high-resolution measurements of pH, DO, PAR, EC, discharge, air temperature and water temperature. This combination of high resolution measurements is unprecedented in the literature, and gives insight into the interplay between physical, hydrological and biogeochemical processes that would be hard to gain from manual, spot measurements. The development and validation of robust *in situ* geochemical monitoring tools for cryospheric sciences could have a major impact on our understanding of these remote, yet highly sensitive, ecosystems. This study describes two relatively short term deployments, and future work will look to establish miniaturised chemical analysers as long term monitoring tools in a range of hard-to-access glacial environments. Potentially revealing applications include supraglacial waters (streams and lakes on the surface of the ice sheet), subglacial environments (e.g. boreholes and subglacial lakes) and deployments underneath sea-ice. Robust monitoring platforms have already been developed for these highly inaccessible environments (e.g. the Lake Ellsworth probe [48] and Cryoegg [29]), and future work could see their integration with high performance chemical analysers. In addition to the nitrate analyser discussed here, similar tools are under development for other nutrients (phosphate[49,50] and silicate), trace metals (e.g. dissolved iron) and carbonate system parameters.

Acknowledgements

This research is part of the UK NERC funded project DELVE (NERC grant NE/I008845/1). We thank Andrew Tedstone, Jon Telling, Ashley Dubnick, David Chandler, Jade Hatton, Marek Stibal, Tyler Kohler, Jakub Žárský and all those who assisted with fieldwork at KS and LG. We also thank Chris Cardwell, David Owsianka, Gregory Slavik and other members of the Ocean Technology and Engineering Group (OTEG) at NOC.

Supporting Information Available

Supporting information contains data from analysis of supraglacial meltwater samples at KS, details on discharge measurements at KS and LG, details on LOD and calibration of the LOC sensor, and plots of the relationship between the LOC sensor measurements at Leverett glacier and the data from the analysis of the manually collected samples

This information is available free of charge via the Internet at http://pubs.acs.org

Figures

Figure 1: Map of deployment sites, showing A) the locations of the nitrate sensor (red star), gauging station (black triangle) and oxygen optode (black circle), in relation to Kiattuut Sermiat, Narsarsuaq and the fjord, and B) the site of the LOC sensor (red star) and gauging station (black triangle) at Leverett Glacier.

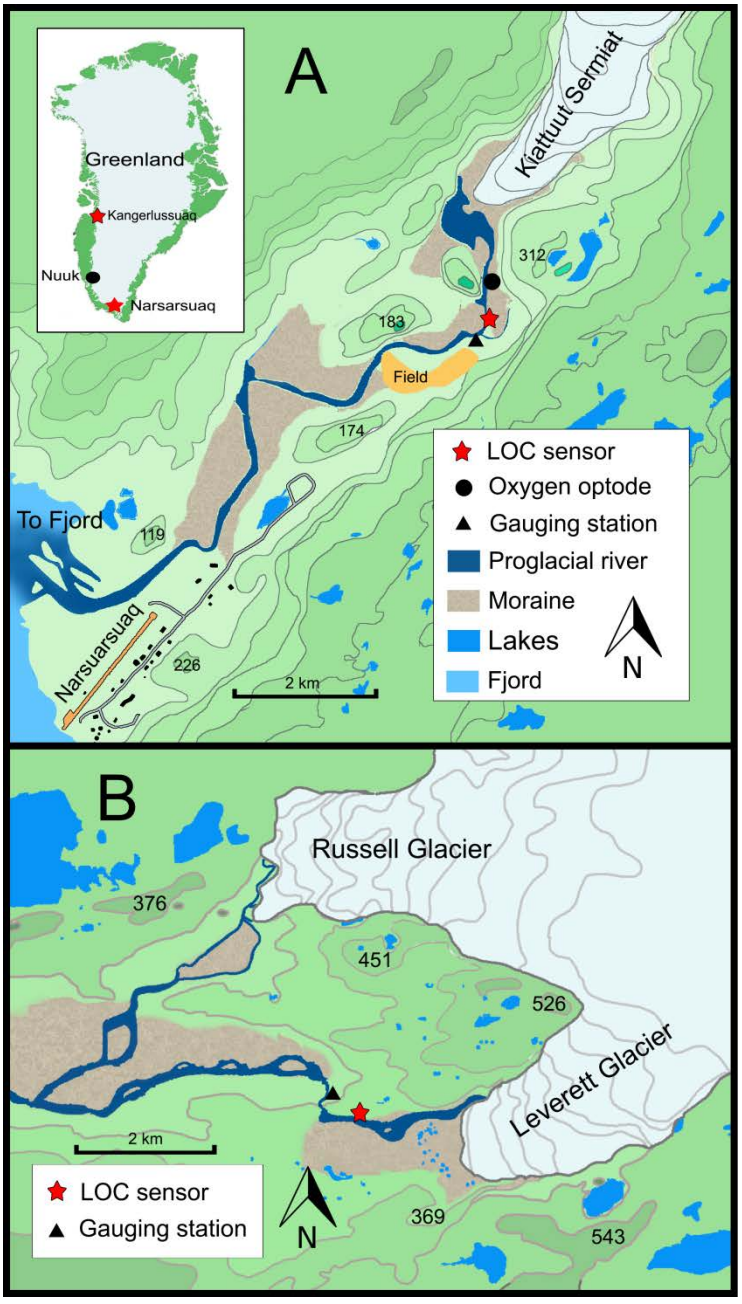

Figure 2: Photographs of the deployment sites showing: A) The proglacial stream at Kiattuut Sermiat with the glacier in the background (the LOC analyser was stationed close to the rocks in the foreground), B) The sensor head that was placed into the proglacial stream. The cross-flow filter inlet was connected to Tygon tubing which led up to the lift pump and LOC analyser located on the riverbank. Also visible are the Honeywell Durafet pH probe and the Campbell Scientific conductivity/temperature probe. C) The sensor deployment site at Leverett Glacier with the glacier in the background. D) The LOC sensor

submerged in the proglacial stream at Leverett Glacier, with the fluid storage bags just visible above the waterline.

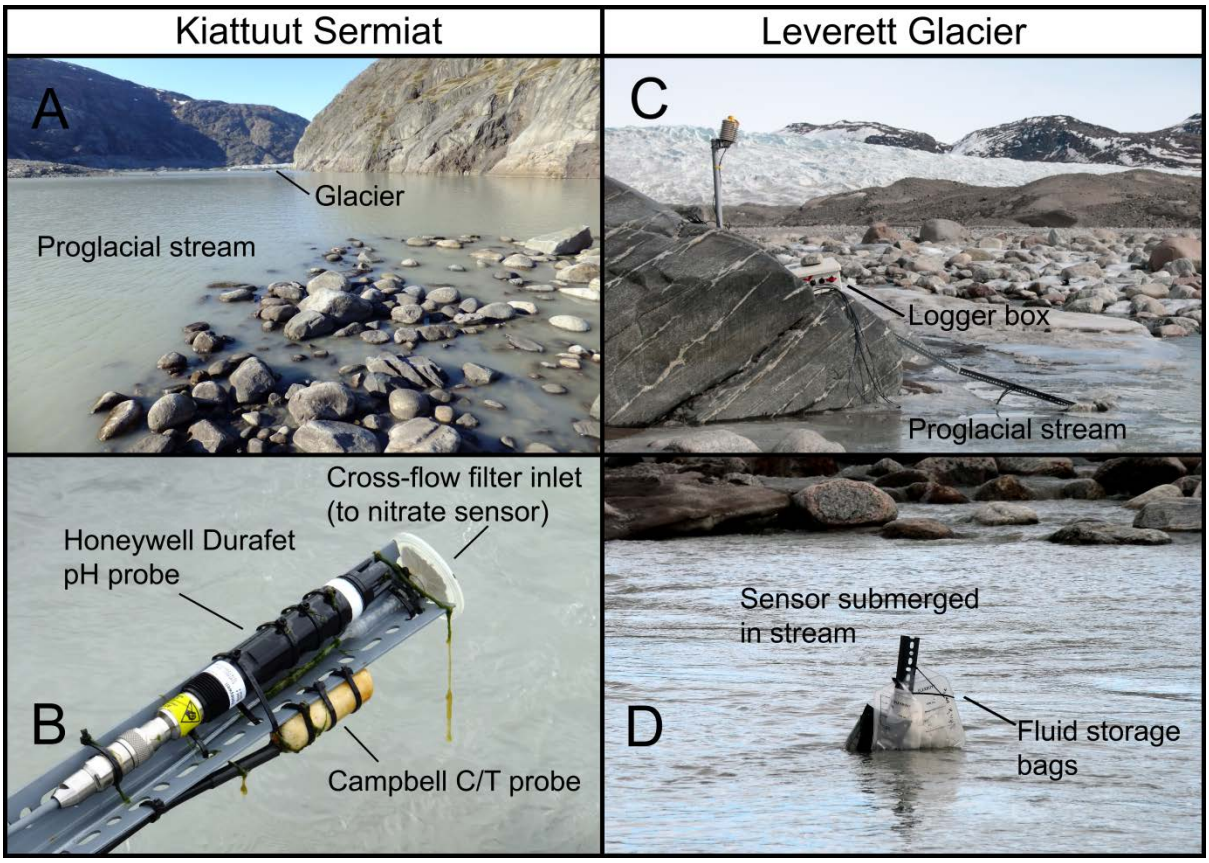

Figure 3: Time series data for all measured parameters at Kiattuut Sermiat glacier, Narsarsuaq, showing: A) Nitrate plus nitrite data from the LOC analyser (blue circles) and manually collected samples analysed using ion chromatography (green circles) and colorimetry (green triangles) as well as discharge (red line). B) Water temperature (blue line) and air temperature (green line). C) Electrical conductivity (blue line) and dissolved oxygen saturation (green line). D) pH (blue line) and PAR (grey line).

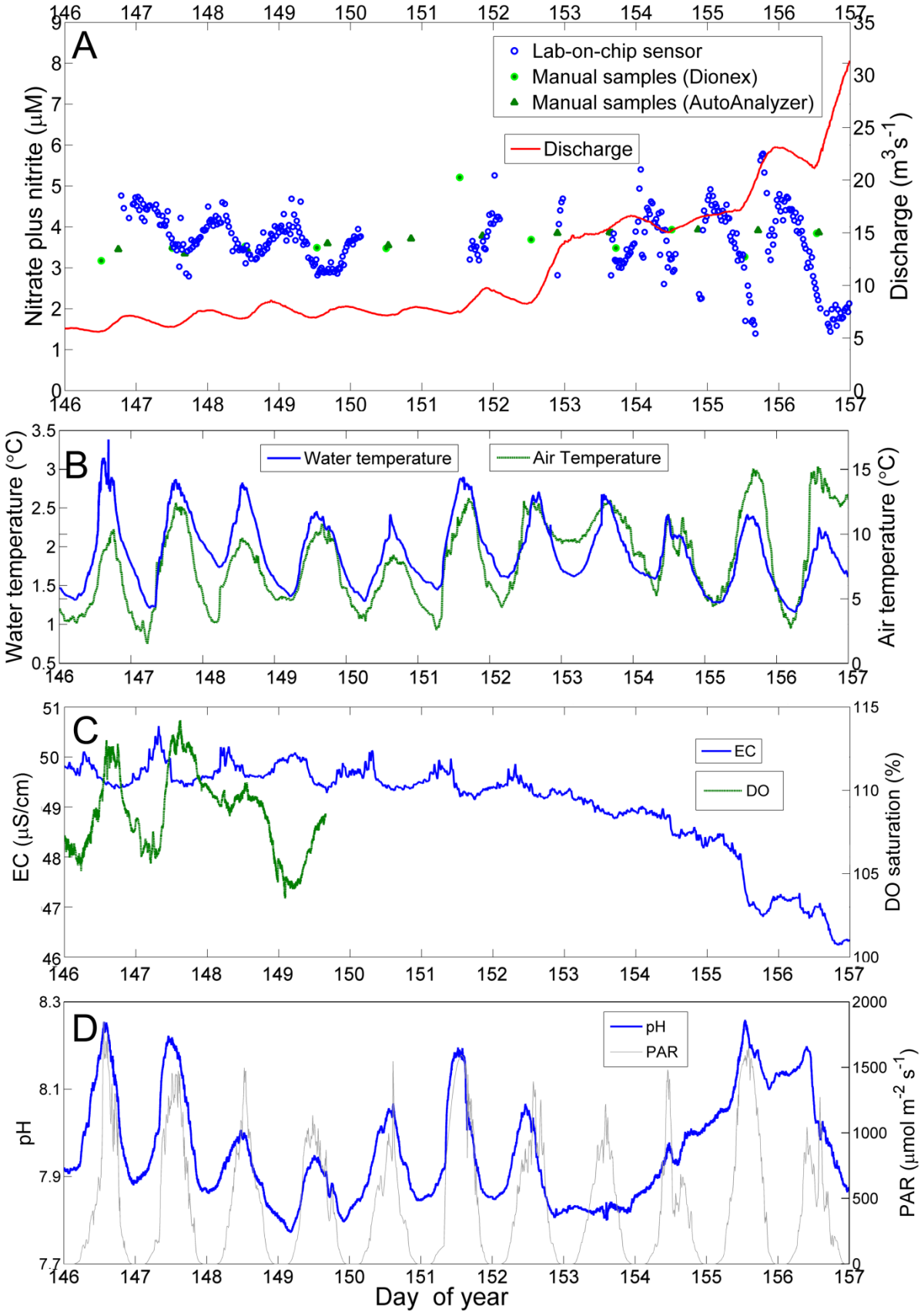
A
Lab-on-chip sensor
Manual samples (Dionex)
Manual samples (AutoAnalyzer)
Discharge
Nitrate plus nitrite (μM)
Discharge (m3s-1)
B
Water temperature
Air Temperature
Water temperature (°C)
Air temperature (°C)
C
EC
DO
EC (μS/cm)
DO saturation (%)
D
pH
PAR
pH
PAR (μmol m-2 s-1)
Day of year

385

Figure 4: Time series data from the deployment of the LOC nitrate sensor at Leverett Glacier showing A) Nitrate plus nitrite data from the LOC analyser (blue circles), manually collected samples that were frozen and analysed colorimetrically (dark green circles) and discharge (red line). B) Water temperature (blue line) and air temperature (green line). C) Electrical conductivity (blue line) and dissolved oxygen saturation (green line). D: pH (blue line) and PAR (grey line).

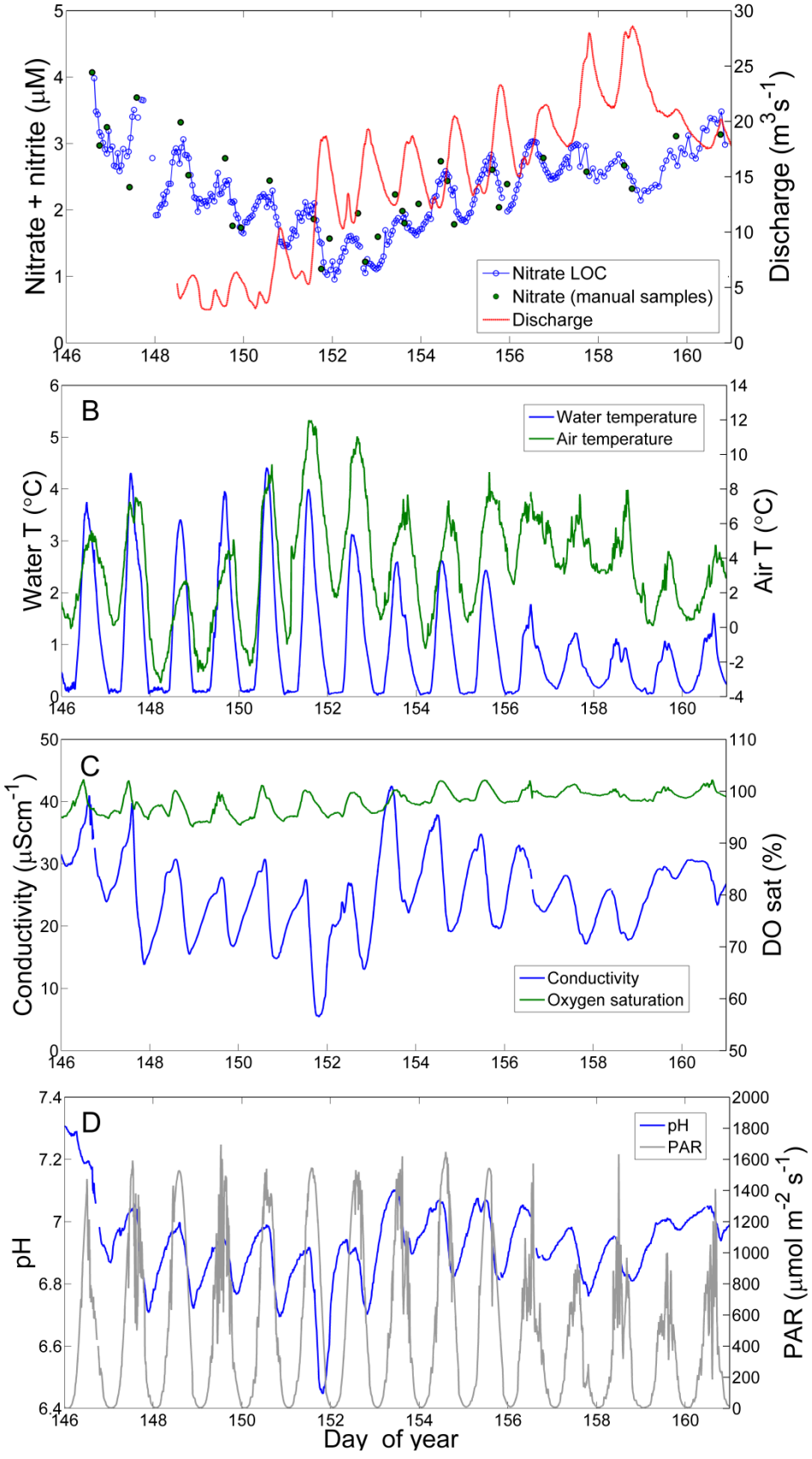
Nitrate + nitrite (µM)
Discharge (m3 s-1)
Nitrate LOC
Nitrate (manual samples)
Discharge
B
Water T (°C)
Air T (°C)
Water temperature
Air temperature
C
Conductivity (µScm-1)
DO sat (%)
Conductivity
Oxygen saturation
D
pH
PAR (µmol m-2 s-1)
pH
PAR
Day of year

391

392

393 **Figure 5:** Plots showing average daily cycles of each of the parameters at KS (red) and LG (blue), created
394 by normalising to daily average, binning into timeslots and plotting the mean normalised value for each
395 timeslot (dots), the median (line) and +/- 1 standard deviation (error bars). Plots shown are A) Nitrate
396 plus nitrite, B) Dissolved oxygen saturation, C) PAR, D) Water temperature, E) Discharge, F) pH, G)

Electrical conductivity, H) Air temperature.

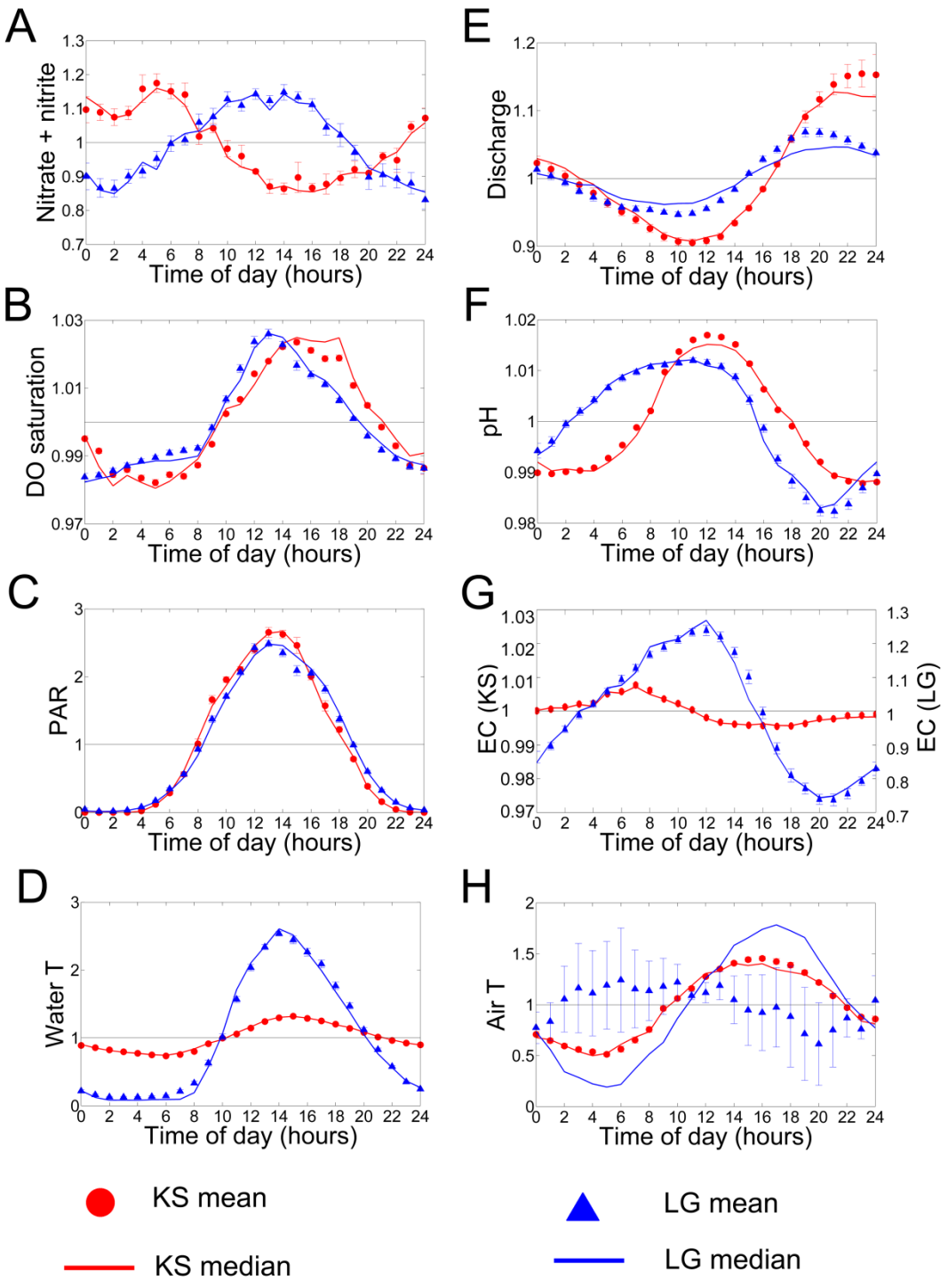

References

(1) Telling, J.; Anesio, A. M.; Tranter, M.; Irvine-Fynn, T.; Hodson, A.; Butler, C.; Wadham, J. Nitrogen fixation on Arctic glaciers, Svalbard. *J. Geophys. Res.* **2011**, *116*, 2–9 DOI: 10.1029/2010JG001632.

(2) Telling, J.; Stibal, M.; Anesio, A. M.; Tranter, M.; Nias, I.; Cook, J.; Bellas, C.; Lis, G.; Wadham, J. L.; Sole, A.; et al. Microbial nitrogen cycling on the Greenland Ice Sheet. *Biogeosciences* **2012**, *9*, 2431–2442 DOI: 10.5194/bg-9-2431-2012.

(3) Wynn, P.; Hodson, A.; Heaton, T.; Chenery, S. Nitrate production beneath a High Arctic glacier, Svalbard. *Chem. Geol.* **2007**, *244* (1–2), 88–102 DOI: 10.1016/j.chemgeo.2007.06.008.

(4) Boyd, E. S.; Lange, R. K.; Mitchell, A. C.; Havig, J. R.; Hamilton, T. L.; Lafrenière, M. J.; Shock, E. L.; Peters, J. W.; Skidmore, M. Diversity, abundance, and potential activity of nitrifying and nitrate-reducing microbial assemblages in a subglacial ecosystem. *Appl. Environ. Microbiol.* **2011**, *77* (14), 4778–4787 DOI: 10.1128/AEM.00376-11.

(5) Wadham, J. L.; Hawkings, J.; Telling, J.; Chandler, D.; Alcock, J.; Lawson, E.; Kaur, P.; Bagshaw, E. A.; Tranter, M.; Tedstone, A.; et al. Sources, cycling and export of nitrogen on the Greenland Ice Sheet. *Biogeosciences* **2016**, *13* (22), 1–30 DOI: 10.5194/bg-2015-484.

(6) Perrette, M.; Yool, A.; Quartly, G. D.; Popova, E. E. Near-ubiquity of ice-edge blooms in the Arctic. *Biogeosciences* **2011**, *8* (2), 515–524 DOI: 10.5194/bg-8-515-2011.

(7) Jensen, H. M.; Pedersen, L.; Burmeister, A.; Hansen, B. W. Pelagic primary production during summer along 65 to 72N off West Greenland. *Polar Biol.* **1999**, *21*, 269–278 DOI: 10.1007/s003000050362.

(8) Hawkings, J. R.; Wadham, J. L.; Tranter, M.; Lawson, E.; Sole, A.; Cowton, T.; Tedstone, A. J.; Bartholomew, I.; Nienow, P.; Chandler, D.; et al. The effect of warming climate on nutrient and solute export from the Greenland Ice Sheet. *Geochemical Perspect. Lett.* **2015**, *1*, 94–104 DOI: 10.7185/geochemlet.1510.

(9) Wadham, J. L.; De'ath, R.; Monteiro, F. M.; Tranter, M.; Ridgwell, a.; Raiswell, R.; Tulaczyk, S. The potential role of the Antarctic Ice Sheet in global biogeochemical cycles. *Earth Environ. Sci. Trans. R. Soc. Edinburgh* **2013**, *104*, 55–67 DOI: 10.1017/S1755691013000108.

(10) Bagshaw, E. A.; Wadham, J. L.; Mowlem, M.; Tranter, M.; Eveness, J.; Fountain, a G.; Telling, J. Determination of dissolved oxygen in the cryosphere: a comprehensive laboratory and field evaluation of fiber optic sensors. *Environ. Sci. Technol.* **2011**, *45* (2),

700–705 DOI: 10.1021/es102571j.

(11) Bagshaw, E. A.; Beaton, A.; Wadham, J. L.; Mowlem, M.; Hawkings, J. R.; Tranter, M. Chemical sensors for in situ data collection in the cryosphere. *TrAC - Trends Anal. Chem.* **2016**, *82*, 348–357 DOI: 10.1016/j.trac.2016.06.016.

(12) Heffernan, J. B.; Cohen, M. J. Direct and indirect coupling of primary production and diel nitrate dynamics in a subtropical spring-fed river. *Limnol. Ocean.* **2010**, *55* (2), 677–688.

(13) Pellerin, B. A.; Downing, B. D.; Kendall, C.; Dahlgren, R. a.; Kraus, T. E. C.; Saraceno, J.; Spencer, R. G. M.; Bergamaschi, B. a. Assessing the sources and magnitude of diurnal nitrate variability in the San Joaquin River (California) with an in situ optical nitrate sensor and dual nitrate isotopes. *Freshw. Biol.* **2009**, *54* (2), 376–387 DOI: 10.1111/j.1365-2427.2008.02111.x.

(14) Pellerin, B. A.; Saraceno, J. F.; Shanley, J. B.; Sebestyen, S. D.; Aiken, G. R.; Wollheim, W. M.; Bergamaschi, B. a. Taking the pulse of snowmelt: in situ sensors reveal seasonal, event and diurnal patterns of nitrate and dissolved organic matter variability in an upland forest stream. *Biogeochemistry* **2011**, *108* (3), 183–198 DOI: 10.1007/s10533-011-9589-8.

(15) Tranter, M.; Brown, G. H.; Hodson, A.; Gurnell, A. M.; Sharp, M. J. Variations in the nitrate concentration of glacial runoff in Alpine and sub-Polar environments. In *Snow and Ice Covers: Interactions with the Atmosphere and Ecosystems (Proceedings of Yokohama Symposia J2 and J5)*; 1994; Vol. 1.

(16) Le Goff, T.; Braven, J.; Ebdon, L.; Scholefield, D. Automatic continuous river monitoring of nitrate using a novel ion-selective electrode. *J. Environ. Monit.* **2003**, *5* (2), 353–358 DOI: 10.1039/b211140n.

(17) Scholefield, D.; Le Goff, T.; Braven, J.; Ebdon, L.; Long, T.; Butler, M. Concerted diurnal patterns in riverine nutrient concentrations and physical conditions. *Sci. Total Environ.* **2005**, *344* (1–3), 201–210 DOI: 10.1016/j.scitotenv.2005.02.014.

(18) Daniel, A.; Birot, D.; Blain, S.; Treguer, P.; Leilde, B.; Menut, E. A submersible flow-injection analyser for the in-situ determination of nitrite and nitrate in coastal waters. *Mar. Chem.* **1995**, *51* (1), 67–77 DOI: 10.1016/0304-4203(95)00052-S.

(19) Gardolinski, P. C. F. C.; David, A. R. J.; Worsfold, P. J. Miniature flow injection analyser for laboratory, shipboard and in situ monitoring of nitrate in estuarine and coastal waters. *Talanta* **2002**, *58* (6), 1015–1027.

(20) Johnson, K.; Sakamoto-Arnold, C.; Beehler, C. Continuous determination of nitrate concentrations in situ. *Deep. Res., Part A* **1989**, *36* (9), 1407–1413 DOI: 10.1016/0198-0149(89)90091-5.

(21) Vuillemin, R.; Le Roux, D.; Dorval, P.; Bucas, K.; Sudreau, J. P.; Hamon, M.; Le Gall, C.; Sarradin, P. M. CHEMINI: A new in situ CHEmical MINIaturized analyzer. *Deep. Res., Part I* **2009**, *56* (8), 1391–1399 DOI: 10.1016/j.dsr.2009.02.002.

(22) Glibert, P. M.; Kelly, V.; Alexander, J.; Codispoti, L. A.; Boicourt, W. C.; Trice, T. M.; Michael, B. In situ nutrient monitoring: A tool for capturing nutrient variability and the antecedent conditions that support algal blooms. *Harmful Algae* **2008**, *8* (1), 175–181 DOI: 10.1016/j.hal.2008.08.013.

(23) Thouron, D.; Vuillemin, R.; Philippon, X.; Lourenço, A.; Provost, C.; Cruzado, A.; Garçon, V. An autonomous nutrient analyzer for oceanic long-term in situ biogeochemical monitoring. *Anal. Chem.* **2003**, *75* (11), 2601–2609.

(24) Snyder, L.; Bowden, W. B. Nutrient dynamics in an oligotrophic arctic stream monitored in situ by wet chemistry methods. *Water Resour. Res.* **2014**, *50* (3), 2039–2049 DOI: 10.1002/2013WR014317.

(25) Beaton, A. D.; Cardwell, C. L.; Thomas, R. S.; Sieben, V. J.; Legiret, F.; Waugh, E. M.; Statham, P. J.; Mowlem, M. C.; Morgan, H. Lab-on-Chip Measurement of Nitrate and Nitrite for In Situ Analysis of Natural Waters. *Environ. Sci. Technol.* **2012**, *46* (17), 9548−9556 DOI: dx.doi.org/10.1021/es300419u.

(26) Nightingale, A. M.; Beaton, A. D.; Mowlem, M. C. Trends in microfluidic systems for in situ chemical analysis of natural waters. *Sensors Actuators B Chem.* **2015**, *221*, 1398–1405 DOI: 10.1016/j.snb.2015.07.091.

(27) Knudsen, N. T.; Yde, J. C.; Gasser, G. Suspended sediment transport in glacial meltwater during the initial quiescent phase after a major surge event at Kuannersuit Glacier, Greenland. *Danish J. Geogr.* **2003**, *107* (1), 1–8.

(28) Hawkings, J.; Wadham, J.; Tranter, M.; Telling, J.; Bagshaw, E.; Beaton, A.; Simmons, S.-L.; Chandler, D.; Tedstone, A.; Nienow, P. The Greenland Ice Sheet as a hot spot of phosphorus weathering and export in the Arctic. *Global Biogeochem. Cycles* **2016**, *30* (2), 191–210 DOI: 10.1002/2015GB005237.

(29) Bagshaw, E. A.; Lishman, B.; Wadham, J. L.; Bowden, J. a.; Burrow, S. G.; Clare, L. R.; Chandler, D. Novel wireless sensors for in situ measurement of sub-ice hydrologic systems. *Ann. Glaciol.* **2014**, *55* (65), 41–50 DOI: 10.3189/2014AoG65A007.

(30) Bartholomew, I.; Nienow, P.; Sole, A.; Mair, D.; Cowton, T.; Palmer, S.; Wadham, J. Supraglacial forcing of subglacial drainage in the ablation zone of the Greenland ice sheet. *Geophys. Res. Lett.* **2011**, *38* (8), 1–5 DOI: 10.1029/2011GL047063.

(31) Beaton, A. D.; Sieben, V. J.; Floquet, C. F. A.; Waugh, E. M.; Abi Kaed Bey, S.; Ogilvie, I. R. G.; Mowlem, M. C.; Morgan, H. An automated microfluidic colourimetric sensor

applied in situ to determine nitrite concentration. *Sens. Actuators, B* **2011**, *156* (2), 1009–1014 DOI: 10.1016/j.snb.2011.02.042.

(32) Yücel, M.; Beaton, A. D.; Dengler, M.; Mowlem, M. C.; Sohl, F.; Sommer, S. Nitrate and Nitrite Variability at the Seafloor of an Oxygen Minimum Zone Revealed by a Novel Microfluidic In-Situ Chemical Sensor. *PLoS One* **2015**, *10*, e0132785 DOI: 10.1371/journal.pone.0132785.

(33) Dubnick, A.; Kazemi, S.; Sharp, M.; Wadham, J.; Hawkings, J.; Beaton, A.; Lanoil, B. Hydrological controls on glacially exported microbial assemblages. *J. Geophys. Res. Biogeosciences* **2017**, *122* (5), 1049–1061 DOI: 10.1002/2016JG003685.

(34) Kohler, T. J.; Žárský, J. D.; Yde, J. C.; Lamarche-Gagnon, G.; Hawkings, J. R.; Tedstone, A. J.; Wadham, J. L.; Box, J. E.; Beaton, A. D.; Stibal, M. Carbon dating reveals a seasonal progression in the source of particulate organic carbon exported from the Greenland Ice Sheet. *Geophys. Res. Lett.* **2017**, *44* (12), 6209–6217 DOI: 10.1002/2017GL073219.

(35) Nimick, D. A.; Gammons, C. H.; Parker, S. R. Diel biogeochemical processes and their effect on the aqueous chemistry of streams: A review. *Chem. Geol.* **2011**, *283* (1–2), 3–17 DOI: 10.1016/j.chemgeo.2010.08.017.

(36) Roberts, B. J.; Mulholland, P. J. In-stream biotic control on nutrient biogeochemistry in a forested stream, West Fork of Walker Branch. *J. Geophys. Res.* **2007**, *112* (G4), G04002 DOI: 10.1029/2007JG000422.

(37) Dokulil, M. T. Potamoplankton and primary productivity in the River Danube. *Hydrobiologia* **2014**, *729*, 209–227 DOI: 10.1007/s10750-013-1589-3.

(38) Johannessen, M.; Henriksen, A. Chemistry of snow melt water: changes in concentration during melting. *Water Resour. Res.* **1978**, *14* (4), 615–619.

(39) Tranter, M.; Brimblecombe, P.; Davies, T. D.; Vincent, C. E.; Abrahams, P. W.; Blackwood, I. The composition of snowfall, snowpack and meltwater in the Scottish highlands-evidence for preferential elution. *Atmos. Environ.* **1986**, *20* (3), 517–525 DOI: 10.1016/0004-6981(86)90092-2.

(40) Sickman, J. O.; Leydecker, A.; Chang, C. C. Y.; Kendall, C.; Melack, J. M.; Lucero, D. M.; Schimel, J. Mechanisms underlying export of N from high-elevation catchments during seasonal transitions. *Biogeochemistry* **2003**, *64*, 1–24 DOI: 10.1023/A:1024928317057.

(41) Tye, A. M.; Heaton, T. H. E. Chemical and isotopic characteristics of weathering and nitrogen release in non-glacial drainage waters on Arctic tundra. *Geochim. Cosmochim. Acta* **2007**, *71* (February), 4188–4205 DOI: 10.1016/j.gca.2007.06.040.

(42) Campbell, D. H.; Clow, D. W.; Ingersoll, G. P.; Mast, M. a.; Spahr, N. E.; Turk, J. T. Processes controlling the chemistry of two snowmelt-dominated streams in the Rocky Mountains. *Water Resour. Res.* **1995**, *31* (11), 2811–2821 DOI: 10.1029/95WR02037.

(43) Hodson, A.; Anesio, A. M.; Tranter, M.; Fountain, A.; Osborn, M.; Priscu, J.; Laybourn-Parry, J.; Sattler, B. Glacial Ecosystems. *Ecol. Monogr.* **2008**, *78* (1), 41–67.

(44) Skidmore, M. L.; Foght, J. M.; Sharp, M. J. Microbial life beneath a high arctic glacier. *Appl. Environ. Microbiol.* **2000**, *66* (8), 3214–3220.

(45) Holloway, J. M.; Dahlgren, R. A.; Hansen, B.; Casey, W. H. Contribution of bedrock nitrogen to high nitrate concentrations in stream water. *Nature* **1998**, *395* (October), 785–788.

(46) Holloway, J. M.; Dahlgren, R. A. Nitrogen in rock: Occurrences and biogeochemical implications. *Global Biogeochem. Cycles* **2002**, *16* (4), 65 1-17 DOI: 10.1029/2002GB001862.

(47) Stevenson, F. J. Chemical state of the nitrogen in rocks. *Geochim. Cosmochim. Acta* **1962**, *26*, 797–809 DOI: https://doi.org/10.1016/0016-7037(62)90040-6.

(48) Mowlem, M.; Saw, K.; Brown, R.; Waugh, E.; Cardwell, C. L.; Wyatt, J.; Magiopoulos, I.; Keen, P.; Campbell, J.; Rundle, N.; et al. Probe technologies for clean sampling and measurement of subglacial lakes. *Philos. Trans. R. Soc. London A Math. Phys. Eng. Sci.* **2015**, *374* (2059) DOI: 10.1098/rsta.2015.0267.

(49) Clinton-Bailey, G. S.; Grand, M. M.; Beaton, A. D.; Nightingale, A. M.; Owsianka, D. R.; Slavik, G. J.; Connelly, D. P.; Cardwell, C. L.; Mowlem, M. C. A Lab-on-Chip Analyzer for in Situ Measurement of Soluble Reactive Phosphate: Improved Phosphate Blue Assay and Application to Fluvial Monitoring. *Environ. Sci. Technol.* **2017**, *51*, 9989−9995 DOI: 10.1021/acs.est.7b01581.

(50) Grand, M. M.; Clinton-Bailey, G. S.; Beaton, A. D.; Schaap, A. M.; Johengen, T. H.; Tamburri, M. N.; Connelly, D. P.; Mowlem, M. C.; Achterberg, E. P. A Lab-On-Chip Phosphate Analyzer for Long-term In Situ Monitoring at Fixed Observatories : Optimization and Performance Evaluation in Estuarine and Oligotrophic Coastal. *Front. Mar. Sci.* **2017**, *4* DOI: 10.3389/fmars.2017.00255.